Electronic Supplementary Material (ESI) for RSC Advances.

3D lanthanide metal organic frameworks constructed from lanthanide formate skeleton and 3,5-bis(4'-carboxy-phenyl)-1,2,4-triazole connector: synthesis, structure and luminescence

Shengyan Wang[a], Jianing Xu[a], Yong Fan[a], Jia Jia[a], Lijuan Gao[a], Jing Sun[a], Liang Shan[a], Xiaodong Chen[a], Li Wang[a,*], Hyo JinSeo[b,*]

Table of contents

Materials and measurements

All commercially available reagents and starting materials were of reagent-grade quality and used without further purification. Powder X-ray diffraction (PXRD) data were obtained using SHIMADAZU XRD-6000 diffractometer with Cu-Kα radiation (λ=1.5418Å), with the step size and the count time of 0.02° and 4s, respectively. Elemental analysis was carried out on an elementary Vario EL cube elemental analyzer. Inductively coupled plasma spectroscopy (ICP) was performed on a OPTIMA 3300DV (Perkin Elmer) spectrometer. FT–IR spectra were recorded on a Nicolet Impact 410 spectrometer between 4000 and 400 cm^{-1} using the KBr pellet method. Thermo gravimetric analysis (TGA) was conducted with a Perkin-Elmer TGA 7 thermo gravimetric analyzer at a heating rate of 10 $°C·min^{-1}$ from room temperature to 800 °C under nitrogen atmosphere. UV−vis absorption spectra were collected on a Perkin-Elmer Lambda 950 spectrophotometer. Photoluminescence analyses were performed on an Edinburgh Instrument FLS920 luminescence spectrometer. The lifetimes were measured at room temperature on FLS920 steady-state and time-resolved fluorescence spectrometer (Edinburgh Instrument). The quantum yields of the solid-state samples were determined at room temperature using an integrating sphere (150 mm diameter, $BaSO_4$ coating) on Edinburgh Instrument FLS920 spectrometer and acquired by the following formula[1]

$$\Phi_{overall} = \frac{A_H}{R_{ST} - R_H}$$

where A_H is the area under emission spectrum of the sample and R_{ST} and R_H are diffuse reflectance of the reflecting standard and the sample, respectively.

Reference:

1. H. B. Zhang, X. C. Shan, Z. J. Ma, L. J. Zhou, M. J. Zhang, P. Lin, S. M. Hu, E. Ma, R. F. Li and S. W. Du, *J. Mater. Chem. C*, 2014, **2**, 1367.

Syntheses

Synthesis of $[Tb_2(HCOO)_2(bct)_2]\cdot H_2O$ (1-Tb) A mixture of $Tb(NO_3)_3$ (0.03 g, 0.067 mmol), H_2bct (0.04 g, 0.129 mmol), DMF (6 ml) and H_2O (4 ml) was adjust to pH = 4 with 6M HNO_3. The mixture was further stirred for 30 min and heated in a 23 ml Teflon-lined stainless steel vessel autoclave at 170 ^oC for 3 d. Colorless block crystals of **1-Tb** suitable for single crystal X-ray diffraction analysis were obtained from the final reaction system by filtration, washed several times with DMF, and dried in air at ambient temperature. (Yield: 63% based on Tb). Elemental analysis for $C_{34}H_{22}N_6O_{13}Tb_2$ (1040.42): C, 39.21; H, 2.11; N, 8.07%. Found: C, 38.95; H, 2.08; N, 7.92%.

Synthesis of $[Eu_2(HCOO)_2(bct)_2]\cdot H_2O$ (2-Eu) A procedure similar to that of **1-Tb** was applied to prepare **2-Eu** except that $Tb(NO_3)_3$ was replaced by $Eu(NO_3)_3$. Colorless block crystals of **2-Eu** were collected from the final reaction system by filtration, washed several times with DMF, and dried in air at ambient temperature. (Yield: 60% based on Eu). Elemental analysis for $C_{34}H_{22}N_6O_{13}Eu_2$ (1026.51): C, 39.74; H, 2.14; N, 8.18%. Found: C, 39.36; H, 2.50; N, 8.56 %.

Synthesis of $[Gd_2(HCOO)_2(bct)_2]\cdot H_2O$ (3-Gd) A procedure similar to that of **1-Tb** was applied to prepare **3-Gd** except that $Tb(NO_3)_3$ was replaced by $Gd(NO_3)_3$. Colorless block crystals of **3-Gd** obtained from the final reaction system by filtration, washed several times with DMF, and dried in air at ambient temperature. (Yield: 60% based on Gd). Elemental analysis for $C_{34}H_{22}N_6O_{13}Gd_2$ (1037.06): C, 39.34; H, 2.12; N, 8.10%. Found: C, 38.97; H, 2.52; N, 8.43 %.

Synthesis of Eu^{3+}-doped 1-Tb A similar process was employed to prepare Eu^{3+}-doped **1-Tb** by adding a certain amount of $Eu(NO_3)_3\cdot 6H_2O$. In a typical doping experiment, the total molar amounts of Eu^{3+} and Tb^{3+} were kept the same as that for **1-Tb**, and the doped Eu^{3+} molar amounts equal to 0.02, 0.1, 0.3, 0.4, 0.5, 1.0, 1.5, 2.0, 5.0 and 10.0% with respect to the total molar amounts.

Synthesis of Eu^{3+}, Tb^{3+}-doped 3-Gd A similar process was employed to prepare Tb^{3+}, Eu^{3+}-doped **3-Gd** by adjusting the co-doping ratio of Tb^{3+}, Eu^{3+} and Gd^{3+} ions and the total molar amounts of Eu^{3+}, Tb^{3+} and Gd^{3+} were kept the same as that for **3-Gd**. In a typical doping experiment, the molar ratios of three Ln^{3+} ions in Tb^{3+}, Eu^{3+}-doped **3-Gd** matches well with that of the starting materials, as further confirmed by inductively coupled plasma (ICP) spectroscopy.

X-ray crystallography

The crystallographic data for **1-Tb** and **3-Gd** were collected on a Siemens Smart CCD diffractometer with graphite-monochromated Mo-Kα (0.71073Å) radiation at a temperature of 293(2) K. No significant decay was observed during the data collection. Data processing was accomplished with the RAPID AUTO processing program. The structure was solved by direct method and refined by full-matrix least-squares on F^2 using the SHELXTL crystallographic software package.[1] All the lanthanide atoms were located first, and then the oxygen and carbon atoms were subsequently found in the difference Fourier maps. All non-hydrogen atoms were refined with anisotropic displacement parameters. The hydrogen atoms attached to free O1 atoms cannot be found in the difference Fourier maps. All structures were examined using the Addsym subroutine of PLATON[2] to assure that no additional symmetry could be applied to the models. Details of the crystal parameters, data collection, and refinements for **1-Tb** and **3-Gd** are summarized in Table S1, while the selected bond lengths and angles are presented in Table S2. Due to their poor quality, single crystals of **2-Eu** cannot be used for single-crystal X-ray diffraction analysis. However, powder X-ray diffraction analysis shows it has the same structure as **1-Tb** and **3-Gd**. Its formula was determined by the elemental and thermogravimetric analysis. CCDC 1011116 and 1428248 contains the supplementary crystallographic data for this paper. These data can be obtained free of charge at www.ccdc.cam.ac.uk [or from the Cambridge Crystallographic Data Centre, 12 Union Road, Cambridge CB2 1EZ, UK; Fax: (Internat.) +44 1223/336 033; E-mail: deposit@ccdc.cam.ac.uk].

Reference

1 G. M. Sheldrick, SHELXS-97, Program for the Solution of Crystal Structures, 1997; G. M. Sheldrick, SHELXL-97, Program for the Refinement of Crystal Structures, 1997.

2 L. Spek, Implemented as the PLATON Procedure, a Multipurpose Crystallographic Tool, 1998.

Table S1. Crystal data and structure refinement for **1** and **3**.

Empirical formula	$C_{34}H_{22}N_6O_{13}Tb_2$	$C_{34}H_{22}N_6O_{13}Gd_2$
Formula weight	1040.42	1037.06
Temperature (K)	293(2)	293(2)
Wavelength (Å)	0.71073	0.71073
Crystal system	orthorhombic	orthorhombic
Space group	*P*nma	*P*nma
a (Å)	6.7445(4)	6.7503(4)
b (Å)	36.3810(19)	36.407(3)
c (Å)	13.0378(7)	13.0761(9)
α (^{o})	90	90
β (^{o})	90	90
γ (^{o})	90	90
Volume (Å^3)	3199.1(3)	3213.6(4)
Z	4	4
Calculated density (Mg/m^3)	2.156	2.139
Absorption coefficient (mm^{-1})	4.469	4.175
F(000)	1999	1991
Theta range for data collection (^{o})	1.12 - 25.02	1.65 - 25.32
Limiting indices	-8<=h<=6, -43<=k<=39, -15<=l<=14	-7<=h<=8, -43<=k<=40, -15<=l<=15
Reflections collected / unique	16883 / 2858 [R_{int}= 0.0684]	17349 / 2956 [R(int) = 0.0977]
Completeness to theta = 25.00	99.7 %	99.0 %
Refinement method	Full-matrix least-squares on F^2	Full-matrix least-squares on F^2
Data / restraints / parameters	2858 / 0 / 253	2956 / 0 / 254
Goodness-of-fit on F^2	1.393	1.101
Final R indices [I>2sigma(I)]	$R_1 = 0.0491$, $wR_2 = 0.1293$	$R_1 = 0.0456$, $wR_2 = 0.0903$
R indices (all data)	$R_1 = 0.0601$, $wR_2 = 0.1460$	$R_1 = 0.0649$, $wR_2 = 0.0959$
Largest diff. peak and hole (eA^{-3})	2.381 and -2.863	1.470 and -1.859

Table S2 Selected Bond lengths [Å] and angles [°] for **1** and **3**.

1			
Tb(1)-O(6)	2.279(7)	Tb(1)-O(5)	2.288(7)
Tb(1)-O(7)	2.331(7)	Tb(1)-O(4)	2.343(7)
Tb(1)-O(2)	2.374(7)	Tb(1)-O(10)^{a}	2.487(7)
Tb(1)-O(2)^{b}	2.507(7)	Tb(1)-O(10)^{b}	2.589(7)
O(2)^{b}-Tb(1)-O(10)^{b}	50.5(2)	O(6)-Tb(1)-O(5)	80.1(3)
O(6)-Tb(1)-O(7)	102.2(3)	O(5)-Tb(1)-O(7)	143.5(3)
O(6)-Tb(1)-O(4)	96.9(3)	O(5)-Tb(1)-O(4)	75.9(3)
O(7)-Tb(1)-O(4)	138.4(3)	O(6)-Tb(1)-O(2)	77.9(3)
O(5)-Tb(1)-O(2)	138.4(2)	O(7)-Tb(1)-O(2)	76.0(3)
O(4)-Tb(1)-O(2)	72.3(3)	O(6)-Tb(1)-O(10)^{a}	76.7(2)
O(5)-Tb(1)-O(10)^{a}	73.1(2)	O(7)-Tb(1)-O(10)^{a}	72.2(2)
O(4)-Tb(1)-O(10)^{a}	148.9(2)	O(2)-Tb(1)-O(10)^{a}	133.5(3)
O(6)-Tb(1)-O(2)^{b}	151.9(2)	O(5)-Tb(1)-O(2)^{b}	120.2(3)
O(7)-Tb(1)-O(2)^{b}	73.6(3)	O(4)-Tb(1)-O(2)^{b}	72.3(3)
O(2)-Tb(1)-O(2)^{b}	74.2(3)	O(10)^{a}-Tb(1)-O(2)^{b}	125.6(2)
O(6)-Tb(1)-O(10)^{b}	157.3(2)	O(5)-Tb(1)-O(10)^{b}	80.1(2)
O(7)-Tb(1)-O(10)^{b}	87.5(2)	O(4)-Tb(1)-O(10)^{b}	88.8(3)
O(2)-Tb(1)-O(10)^{b}	124.6(2)	O(10)^{a}-Tb(1)-O(10)^{b}	87.09(13)

Symmetry transformations used to generate equivalent atoms:

a -x-1/2,-y+2,z+1/2 b -x,-y+2,-z+1

3			
Gd(1)-O(1)	2.285(5)	Gd(1)-O(7)^{b}	2.298(5)
Gd(1)-O(2)	2.344(5)	Gd(1)-O(4)	2.348(5)
Gd(1)-O(5)	2.382(5)	Gd(1)-O(6)	2.500(5)
Gd(1)-O(5)^{a}	2.531(5)	Gd(1)-O(6)^{b}	2.587(5)
O(1)-Gd(1)-O(7)^{b}	79.92(18)	O(1)-Gd(1)-O(2)	102.38(18)
O(7)^{b}-Gd(1)-O(2)	143.60(19)	O(1)-Gd(1)-O(4)	97.29(19)
O(7)^{b}-Gd(1)-O(4)	75.96(19)	O(2)-Gd(1)-O(4)	138.11(19)
O(1)-Gd(1)-O(5)	77.91(18)	O(7)b-Gd(1)-O(5)	138.17(18)
O(2)-Gd(1)-O(5)	76.22(19)	O(4)-Gd(1)-O(5)	72.28(19)
O(1)-Gd(1)-O(6)	76.49(18)	O(7)^{b}-Gd(1)-O(6)	73.18(18)
O(2)-Gd(1)-O(6)	72.18(18)	O(4)-Gd(1)-O(6)	149.12(18)
O(5)-Gd(1)-O(6)	133.41(19)	O(1)-Gd(1)-O(5)^{a}	152.38(17)
O(7)^{b}-Gd(1)-O(5)^{a}	120.25(18)	O(2)-Gd(1)-O(5)^{a}	73.16(18)
O(4)-Gd(1)-O(5)^{a}	72.36(19)	O(5)-Gd(1)-O(5)^{a}	74.56(19)
O(6)-Gd(1)-O(5)^{a}	125.26(17)	O(1)-Gd(1)-O(6)b	157.08(17)
O(7)^{b}-Gd(1)-O(6)^{b}	80.18(17)	O(2)-Gd(1)-O(6)^{b}	87.16(18)
O(4)-Gd(1)-O(6)^{b}	88.77(19)	O(5)-Gd(1)-O(6)^{b}	124.89(18)
O(6)-Gd(1)-O(6)^{b}	86.96(9)	O(5)^{a}-Gd(1)-O(6)^{b}	50.33(16)

Symmetry transformations used to generate equivalent atoms:

a -x+2,-y+2,-z b x+1/2,y,-z+1/2

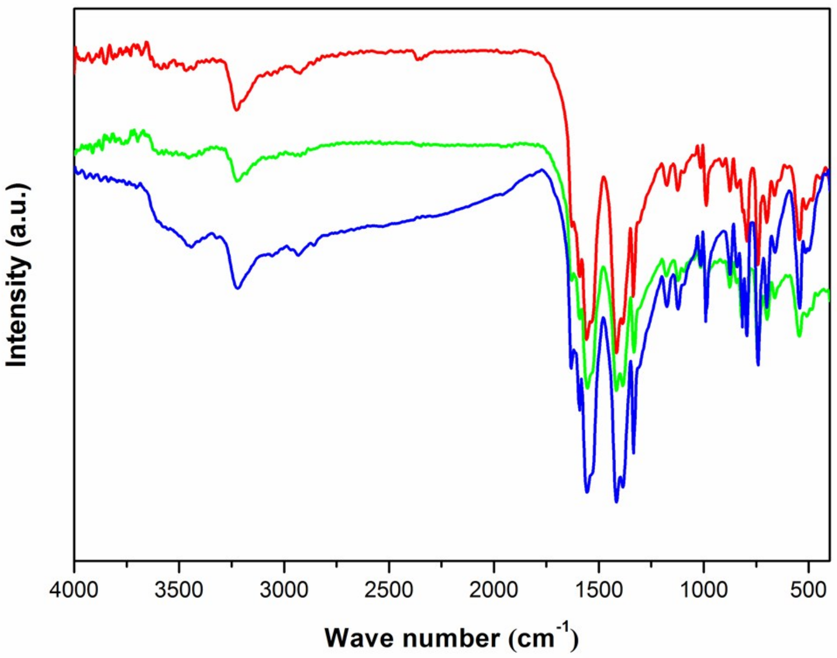

Figure S1 IR spectra of **1**-**3**.

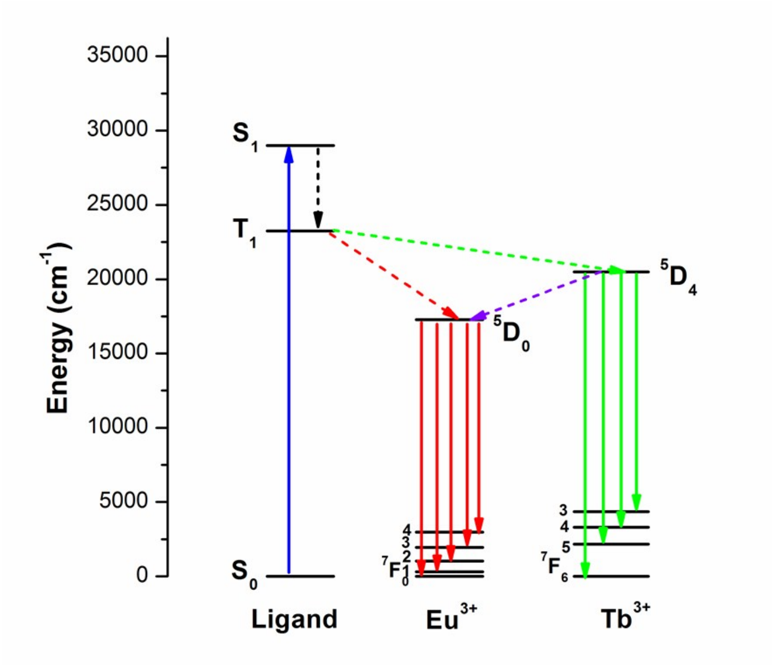

Figure S2 The different energy levels of H_2bct ligand, Eu^{3+} and Tb^{3+} ions and possible energy transfer process.

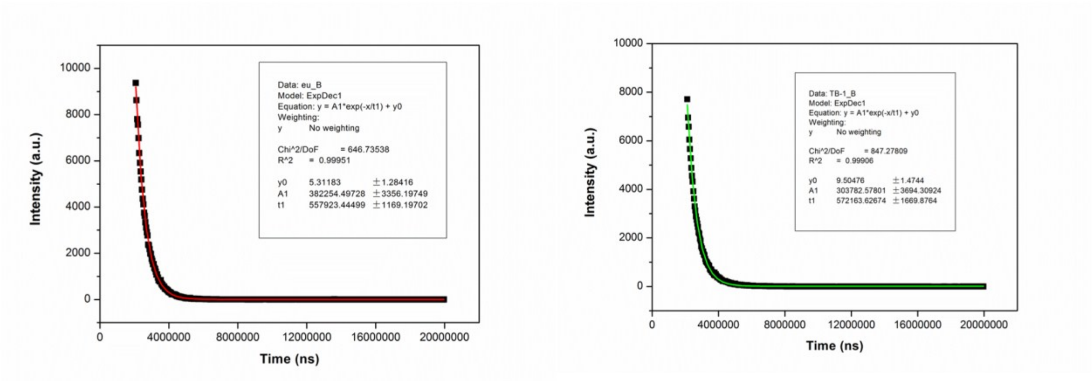

Data: eu_B
Model: ExpDec1
Equation: y = A1*exp(-x/t1) + y0
Weighting:
y No weighting

Chi^2/DoF = 646.73538
R^2 = 0.99951

y0	5.31183	±1.28416
A1	382254.49728	±3356.19749
t1	557923.44499	±1169.19702

Data: TB-1_B
Model: ExpDec1
Equation: y = A1*exp(-x/t1) + y0
Weighting:
y No weighting

Chi^2/DoF = 847.27809
R^2 = 0.99906

y0	9.50476	±1.4744
A1	303782.57801	±3694.30924
t1	572163.62674	±1669.8764

Eu **Tb**

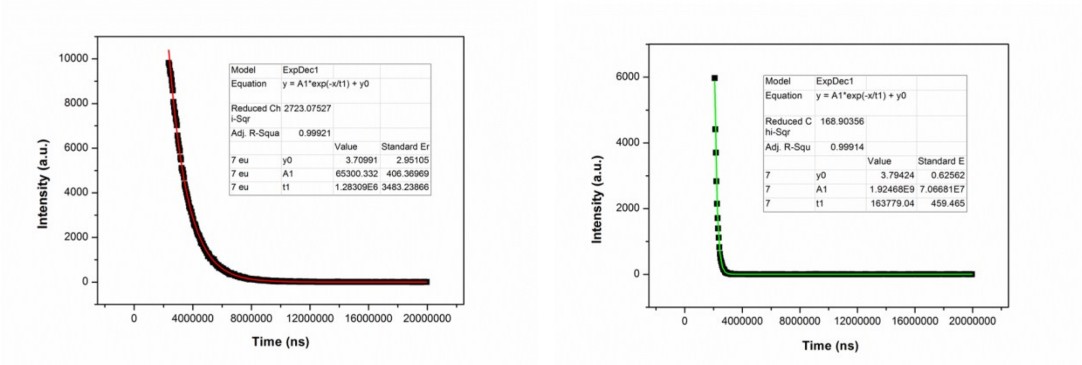

Model	ExpDec1		
Equation	y = A1*exp(-x/t1) + y0		
Reduced Chi-Sqr	2723.07527		
Adj. R-Squa	0.99921		
		Value	Standard Er
7 eu	y0	3.70991	2.95105
7 eu	A1	65300.332	406.36969
7 eu	t1	1.28309E6	3483.23866

Model	ExpDec1		
Equation	y = A1*exp(-x/t1) + y0		
Reduced Chi-Sqr	168.90356		
Adj. R-Squ	0.99914		
		Value	Standard E
7	y0	3.79424	0.62562
7	A1	1.92468E9	7.06681E7
7	t1	163779.04	459.465

Eu0.02Tb0.98 **Eu0.02Tb0.98**

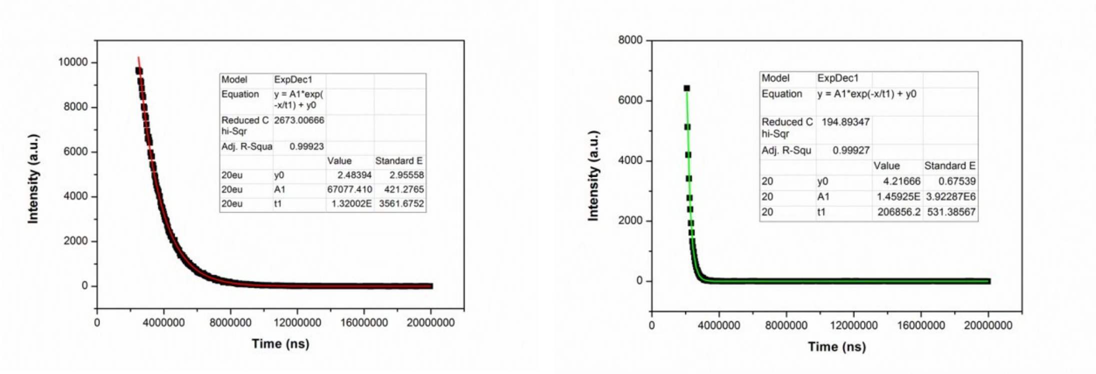

Model	ExpDec1		
Equation	y = A1*exp(-x/t1) + y0		
Reduced Chi-Sqr	2673.00666		
Adj. R-Squa	0.99923		
		Value	Standard E
20eu	y0	2.48394	2.95558
20eu	A1	67077.410	421.2765
20eu	t1	1.32002E	3561.6752

Model	ExpDec1		
Equation	y = A1*exp(-x/t1) + y0		
Reduced Chi-Sqr	194.89347		
Adj. R-Squ	0.99927		
		Value	Standard E
20	y0	4.21666	0.67539
20	A1	1.45925E	3.92287E6
20	t1	206856.2	531.38567

Eu0.01Tb0.99 **Eu0.01Tb0.99**

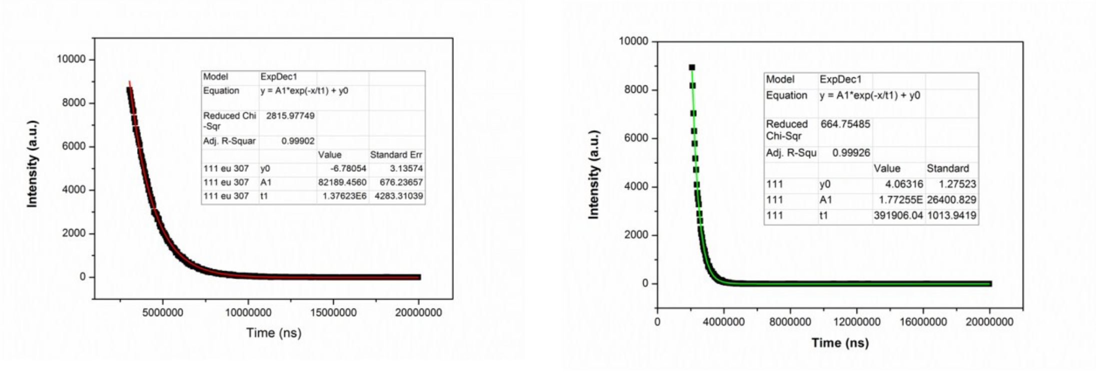

Model	ExpDec1		
Equation	y = A1*exp(-x/t1) + y0		
Reduced Chi-Sqr	2815.97749		
Adj. R-Squar	0.99902		
		Value	Standard Err
111 eu 307	y0	-6.78054	3.13574
111 eu 307	A1	82189.4560	676.23657
111 eu 307	t1	1.37623E6	4283.31039

Model	ExpDec1		
Equation	y = A1*exp(-x/t1) + y0		
Reduced Chi-Sqr	664.75485		
Adj. R-Squ	0.99926		
		Value	Standard
111	y0	4.06316	1.27523
111	A1	1.77255E	26400.829
111	t1	391906.04	1013.9419

Eu0.004Tb0.996 **Eu0.004Tb0.996**

Figure S3 Luminescent decay curves of 1-Tb, 2-Eu, 0.4%, 1% and2% Eu^{3+}-doped 1-Tb

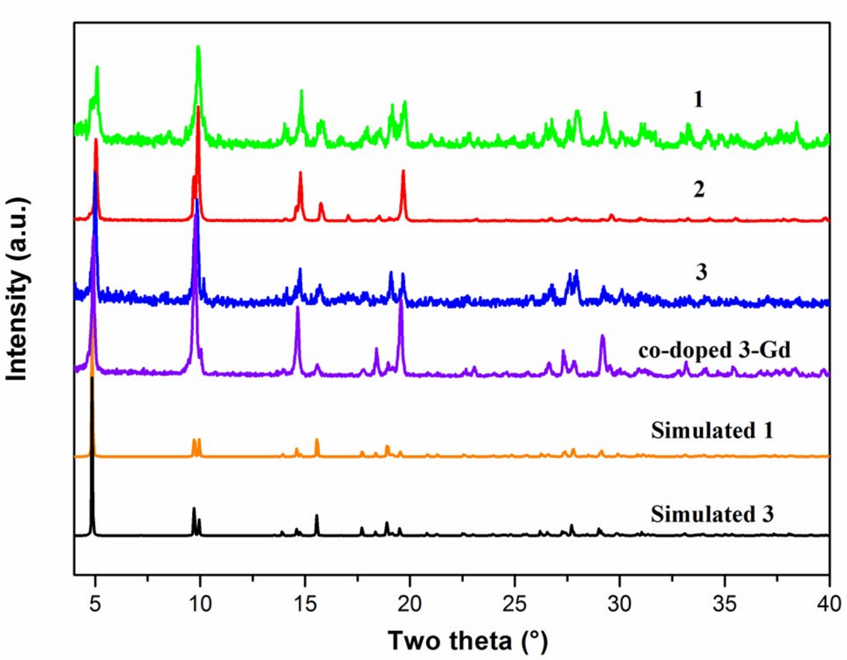

Figure S4 The simulated and experimental PXRD patterns for Ln-MOFs.

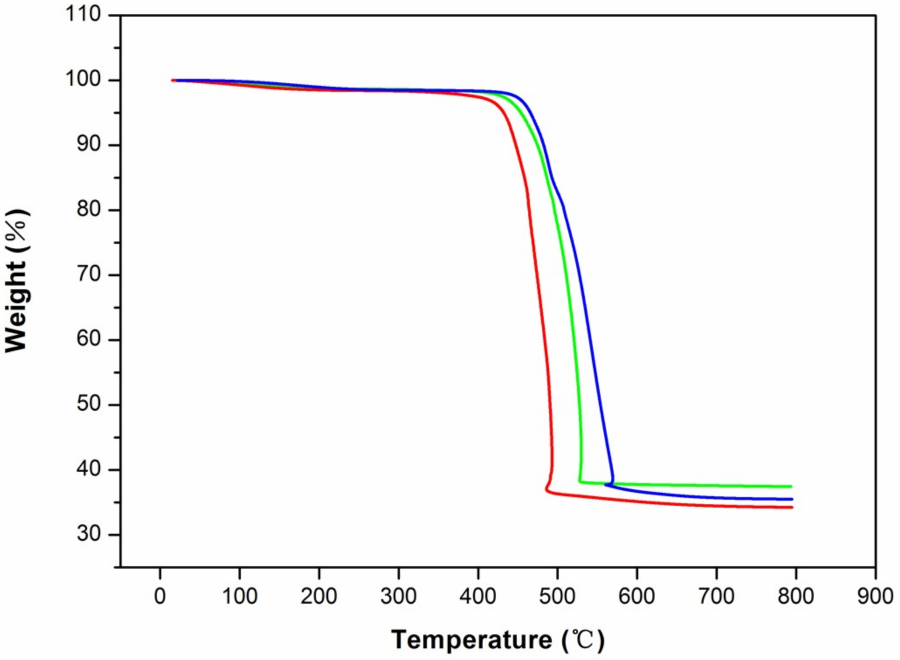

Figure S5 TG curves of **1-3**.

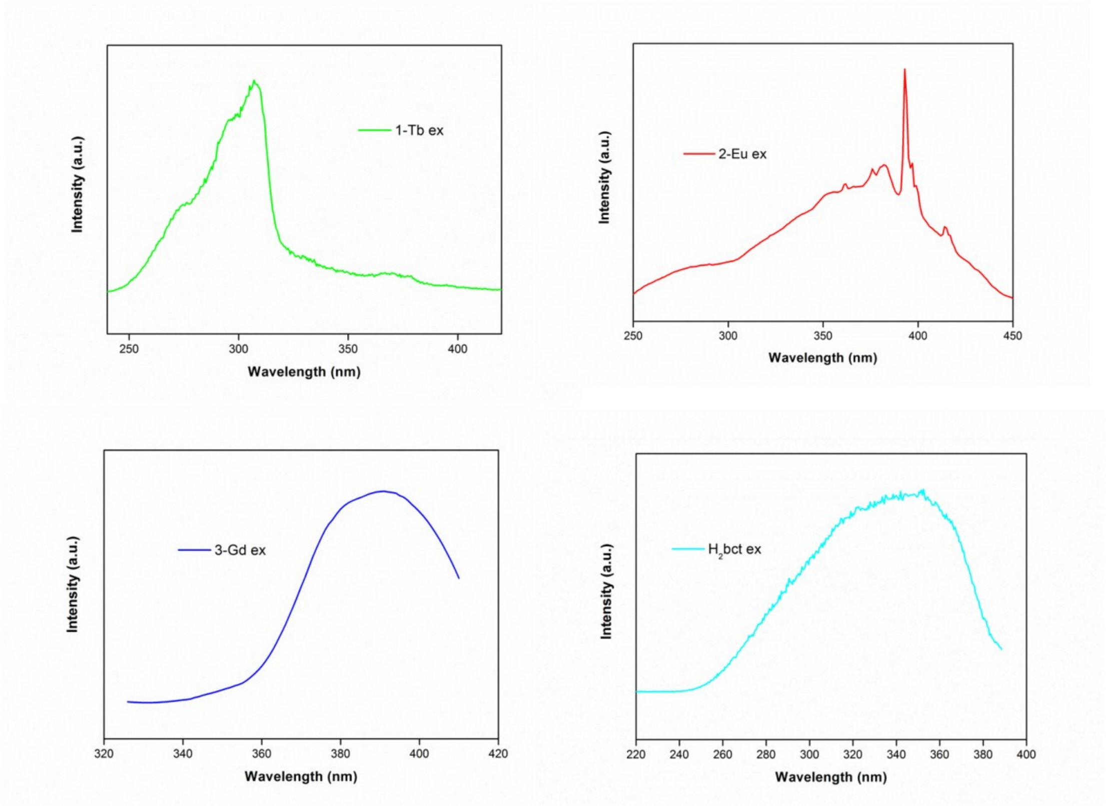

Figure S6 Excitation spectra of **1-3** and H_2bct ligand in the solid state at room temperature.

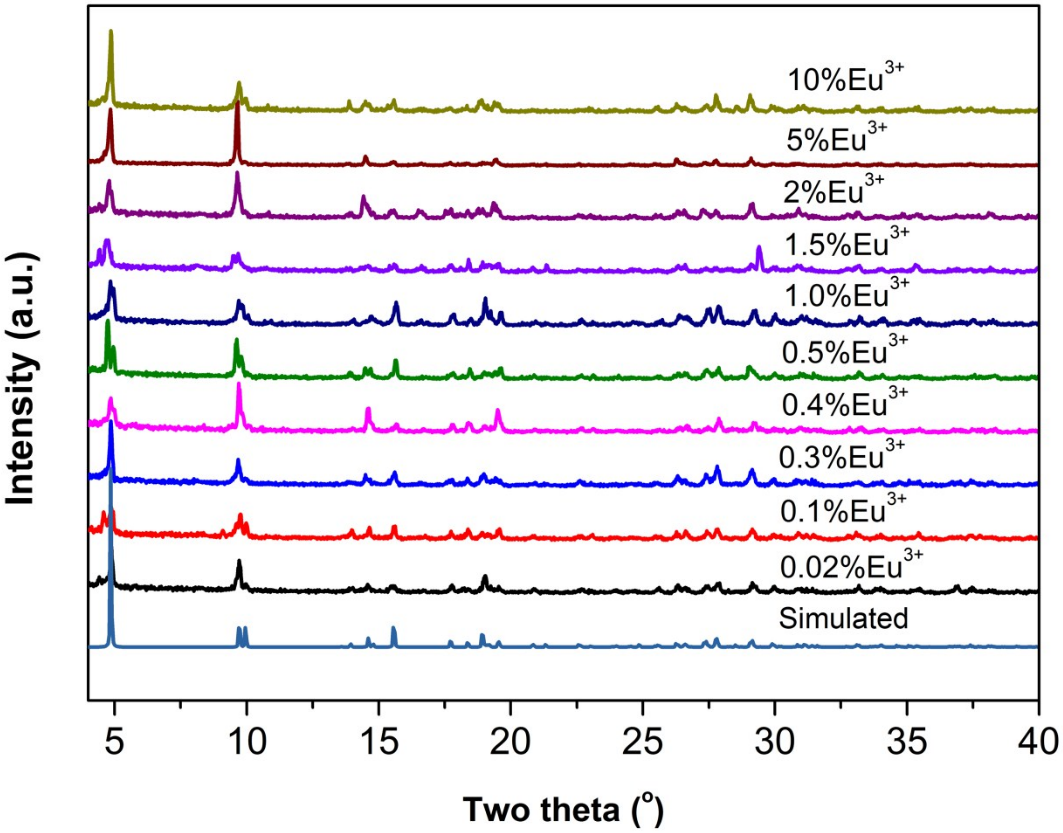

Figure S7 The simulated and experimental PXRD patterns of the Eu^{3+} doped materials.